Academic Journal of Applied Sciences
ISSN: 3105-0549 (Print), ISSN: 3105-0557 (Online) | Vol. 3, No. 3, 2026

Route Optimization of Single-Supply-Point Perishable Goods Multimodal Transport Considering Temperature-Time Spoilage Loss

Hao Yang [1, *], Jie Yang [2]

[1] School of Mathematics and Computers, Panzhihua University, Panzhihua, 617000, China

[2] Middle School Affiliated to Chengdu University, Chengdu, 610057, China

[*] **Corresponding author**: (Email: yhaowss0921@163.com)

Abstract: Perishable goods transported over long multimodal chains face a coupled cost-quality decision because road and rail expose cargo to different temperatures and travel times. This study formulates a bi-objective route optimization model for one supply point and two demand points, integrating transportation, transfer, refrigeration, time-window, and temperature-time spoilage costs. A Q10 deterioration function links mode temperature to product loss, while a piecewise satisfaction function represents delivered quality. Feasible route-mode schemes are generated from k-shortest paths and then combined globally by NSGA-II. Exact enumeration validates the formulation on a ten-node network, and sensitivity analysis evaluates the kinetic parameters. The proposed method obtains 100 Pareto solutions with 98.0% coverage of the exact front in 0.81 s; the minimum-cost plan is 21,103.56 CNY with satisfaction 0.8274, whereas the highest-satisfaction plan reaches 0.9652 at higher cost. The results show how temperature sensitivity changes the preferred mode mix and provide a traceable basis for multimodal cold-chain planning.

Keywords: Multimodal Transport, Perishable Goods, Temperature-Time Spoilage, Route Optimization, Bi-Objective Optimization, NSGA-II.

1. Introduction

Perishable goods are increasingly moved across long supply chains, where temperature exposure and handling time jointly determine whether the delivered quantity retains its intended value. Freshness deterioration is therefore a logistics decision variable rather than a post hoc quality check, while multimodal transport introduces a further tension between low-cost rail movement and better-controlled refrigerated road movement [1]. A route that is short or inexpensive can still be unattractive when a warm segment accelerates quality loss, and a quality-oriented route can impose extra transport, transfer, refrigeration, or delay costs [2].

Existing studies have established deterioration-aware inventory and routing models, but their treatment of temperature, mode changes, and quality satisfaction is not uniform. Temperature-dependent kinetics have been used to describe product degradation [1], and routing models have incorporated multimodal path selection, time windows, and mode assignment [3-5]. Recent formulations further show that route choice, carbon considerations, customer value, and quality preservation interact across transport modes [6-10]. However, a compact framework is still needed for a single supply point serving several demand points when each arc may be operated by road or rail, transfers have time and cost consequences, and the deterioration rate changes with the transport temperature. The central research question is how to construct a route-mode decision model that exposes this cost-quality trade-off quantitatively and can return a well-distributed set of feasible alternatives. From a logistics perspective, the decision is not only which path to select but where to transfer and which mode to assign to each arc. These choices determine exposure time, the quantity carried into segments, and arrival-time penalty. A model that reports only one optimum would hide compromises, whereas a Pareto set allows a planner to choose a route after considering cargo value and the preferred quality level. This structure also makes exact enumeration a transparent benchmark for the heuristic.

This paper formulates a bi-objective multimodal route optimization model for one supply point and two demand points. The model combines transport, transfer, refrigeration, time-window, and temperature-time spoilage costs, and represents customer quality through a piecewise satisfaction function. Temperature dependence is introduced through Q10 kinetics, while route continuity, mode uniqueness, transfer limits, arrival times, shelf life, and spoilage accumulation are enforced explicitly. The solution procedure uses a candidate-scheme pool generated from k-shortest paths and feasible route-mode combinations, followed by NSGA-II for the global selection of one scheme per demand point. Exact enumeration on the ten-node test network provides a reference Pareto front, and sensitivity experiments examine the effects of the reference deterioration rate and temperature coefficient. The resulting framework connects physical quality loss with transport decisions, clarifies why cost-minimizing and quality-maximizing plans use different mode mixes, and supplies a reproducible basis for selecting multimodal routes for temperature-sensitive goods.

2. Problem Description and Model

2.1. Network, Assumptions, And Notation

Consider an undirected transport network $G = (N, L)$, where $N = O \cup R \cup D$ contains one supply point O, transfer nodes R, and demand points D, and L is the set of road and rail arcs. Each demand point is served by one unsplit route. Arc distance, mode speed, unit cost, mode temperature,

transfer conditions, demand, soft time windows, and shelf life are deterministic. A route may use road and rail, with no more than Ntr transfers. The notation used in the model is collected in Table 1.

Table 1. Notation of the route optimization model.

Symbol	Definition
N, O, R, D	Set of all nodes, supply point, transfer nodes, demand points
L, K	Set of arcs; set of transportation modes K = {1 (road), 2 (rail)}
Q_d	Demand (tonnage) of demand point d
d_{ij}, v_k, c_{ij}^k	Distance of arc (i,j); speed and unit transport cost of mode k
q_t, τ_t	Transfer (transshipment) cost per ton and transfer time per transfer
W	Unit value of goods (CNY/ton)
c_h	Refrigeration rental cost per ton per hour
c_e, c_f	Early-arrival holding penalty and late-arrival delay penalty per ton per hour
$[E_d, L_d]$	Soft time window of demand point d
θ0, T0, Q10, θ(T)	Reference deterioration rate, reference temperature, temperature coefficient, and temperature-dependent deterioration rate
δ1, δ2	Loss-rate thresholds at which full and zero satisfaction are achieved
a, b	Constants of the satisfaction function
δ_d	Spoilage loss rate of demand point d (defined by (19))
F_d	Satisfaction degree of demand point d (defined by (10))
t_d	Arrival time at demand point d (defined by (17))
S_d	Shelf life of the perishable goods for demand point d
N_{tr}	Maximum number of mode transfers allowed along a route
x_{ij}^{kd}	Binary variable: 1 if the goods of demand point d travel on arc (i,j) by mode k, 0 otherwise
y_i^d	Binary variable: 1 if a mode transfer occurs at node i for demand point d, 0 otherwise

2.2. Cost and Quality Components

The total cost includes transportation, transfer, temperature-time spoilage, refrigeration, and time-window penalty components. Transportation and transfer costs are proportional to demand and arc or transfer use:

$$C_1 = \sum_{d\in D}\sum_{(i,j)\in L}\sum_{k\in K} c_{ij}^k \cdot d_{ij} \cdot Q_d \cdot x_{ij}^{kd} \quad (1)$$

$$C_2 = \sum_{d\in D}\sum_{i\in R} q_t \cdot Q_d \cdot y_i^d \quad (2)$$

The deterioration rate follows Q10 kinetics. For a segment at temperature T, the lost quantity is computed from the exposure time and the remaining quantity is carried to the next segment.

$$\theta(T) = \theta_0 \cdot Q10^{(T-T_0)/10} \quad (3)$$

$$\Delta Q = Q_0 \cdot [1 - e^{-\theta(T)\cdot t}] \quad (4)$$

Summing segment loss, refrigeration, and early- or late-arrival penalties gives the remaining cost components:

$$C_3 = \sum_{d\in D} W \cdot \sum_{(i,j)\in L, k\in K} \Delta Q_{ij}^k \quad (5)$$

$$C_4 = \sum_{d\in D} c_h \cdot Q_d \cdot t_d \quad (6)$$

$$C_5 = \sum_{d\in D} Q_d \cdot [c_e \cdot max(E_d - t_d, 0) + c_f \cdot max(t_d - L_d, 0)] \quad (7)$$

The bi-objective formulation minimizes total cost and maximizes average quality satisfaction. Satisfaction is represented by a piecewise linear function of the route loss rate δd, with full satisfaction below δ1 and zero satisfaction above δ2.

$$minC = C_1 + C_2 + C_3 + C_4 + C_5 \quad (8)$$

$$maxF = \frac{1}{|D|} \cdot \sum_{d\in D} F_d \quad (9)$$

$$F_d = max(0, min(1, a - b \cdot \frac{\delta_d - \delta_1}{\delta_2 - \delta_1})) \quad (10)$$

2.3. Constraints and Decision Variables

The binary variable xijkd selects mode k on arc (i,j) for demand d, yid identifies a transfer at node i, and td is the arrival time. The following constraints impose single departure and termination, flow conservation, mode uniqueness, transfer activation and limits, arrival time, shelf life, spoilage accumulation, and variable domains:

$$\sum_{j\in N}\sum_{k\in K} x_{oj}^{kd} = 1, \forall d \in D \quad (11)$$

$$\sum_{i\in N}\sum_{k\in K} x_{id}^{kd} = 1, \forall d \in D \quad (12)$$

$$\sum_{i\in N}\sum_{k\in K} x_{iv}^{kd} = \sum_{j\in N}\sum_{k\in K} x_{vj}^{kd}, \forall v \in R, \forall d \in D \quad (13)$$

$$\sum_{k\in K} x_{ij}^{kd} \le 1, \forall (i,j) \in L, \forall d \in D \quad (14)$$

$$y_i^d \ge x_{ji}^{kd} + x_{il}^{ld} - 1, \forall i \in R, \forall d \in D, \forall k \ne l \quad (15)$$

$$\sum_{i\in R} y_i^d \le N_{tr}, \forall d \in D \quad (16)$$

$$t_d = \sum_{(i,j)\in L}\sum_{k\in K}(d_{ij}/v_k) \cdot x_{ij}^{kd} + \sum_{i\in R} \tau_t \cdot y_i^d, \forall d \in D \quad (17)$$

$$t_d \le S_d, \forall d \in D \quad (18)$$

$$\delta_d = 1 - \prod_{(i,j)\in L, k\in K} e^{-\theta(T_k)\cdot(d_{ij}/v_k)\cdot x_{ij}^{kd}}, \forall d \in D \quad (19)$$

$$x_{ij}^{kd} \in \{0,1\}, y_i^d \in \{0,1\}, t_d \ge 0 \quad (20)$$

The product form in (19) accumulates the decay of the remaining quantity over the selected route and is equivalent to exponential decay under piecewise-constant mode temperatures. The feasible set therefore keeps route continuity and the quality constraint in the same mathematical system. The overall modelling and solution workflow is summarized in Figure 1.

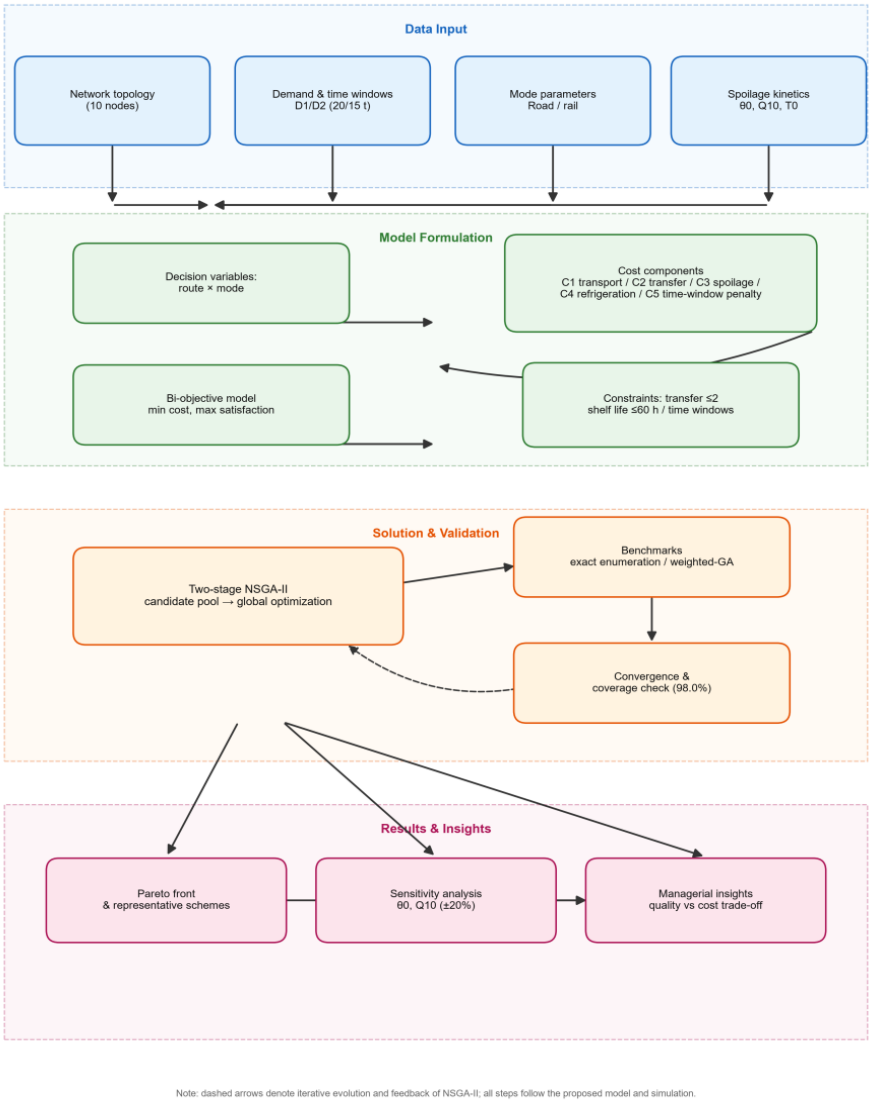


Figure 1. Methodological framework of the perishable multimodal route optimization.

3. Validation and Solution Method

The model is checked by exhaustive enumeration on the test network. There are 96 feasible schemes for D1 and 63 for D2, giving 6,048 combined route-mode choices. Non-dominated sorting produces the exact Pareto front, which provides a reference for the algorithm and verifies the cost-satisfaction trade-off. The resulting validation statistics are summarized in Table 2.

Table 2. Exact enumeration results for model validation.

Item	Value
Feasible combinations enumerated	96 × 63 = 6,048
Pareto-optimal solutions (exact)	27
Minimum total cost (CNY)	21,103.56
Satisfaction at minimum cost	0.8274
Maximum satisfaction	0.9792
Runtime (s)	8.39

3.1. Two-stage NSGA-II

The combinatorial search is decomposed into candidate generation and global combination. The first stage enumerates k-shortest paths and feasible route-mode combinations for each demand point, filtering railway availability, transfer limits, and shelf-life violations. The second stage selects one scheme per demand point with NSGA-II. A chromosome is encoded as (idx1, idx2); decoding returns total cost and average satisfaction. A population of 100 is evolved for 80 generations using non-dominated sorting, crowding distance, binary tournament selection, crossover probability 0.9, mutation probability 0.15, and elitist replacement. The method returns the first non-dominated front in one run. Exact algorithms for time-window routing with perishable products provide a complementary benchmark [10]. The per-generation complexity is $O(I\cdot(N\cdot D\cdot H + N^2))$, while candidate-pool generation is performed once with cost $O(K\cdot H\cdot S)$.

4. Numerical Experiment

4.1. Network and Parameters

A ten-node network is used: node 0 is the supply point, nodes 1-7 are transfer nodes, and nodes 8 and 9 are demand points D1 and D2. The network contains 16 road arcs and 10 rail trunk arcs. D1 and D2 demand 20 t and 15 t, with time windows [24,36] h and [30,48] h. Road transport uses 70 km/h, 0.8 CNY/(t·km), and 5 °C; rail uses 100 km/h, 0.35 CNY/(t·km), and 20 °C. Transfer cost and time are 8 CNY/(t·transfer) and 2 h. The unit value is 3,000 CNY/t, refrigeration costs 0.5 CNY/(t·h), and early- and late-arrival

penalties are 0.5 and 1.0 CNY/(t·h). The kinetic parameters are $\theta 0 = 0.002\ h^{-1}$, T0 = 10 °C, Q10 = 2.0, with thresholds $\delta 1 = 0.02$ and $\delta 2 = 0.15$. The network topology is shown in Figure 2, and the parameter settings are summarized in Table 3.

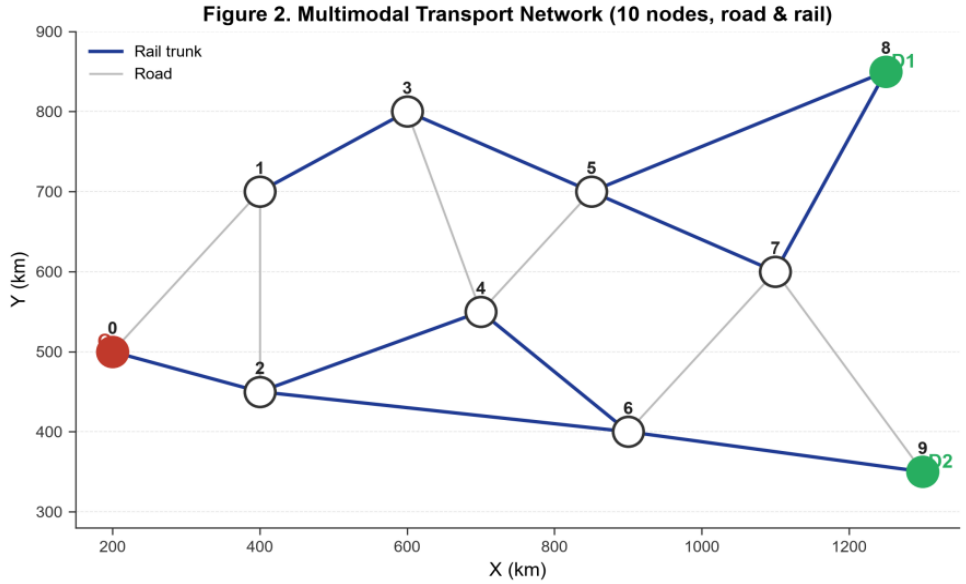


Figure 2. Multimodal transport network with ten nodes, road arcs, and rail arcs.

Table 3. Parameter settings of the numerical experiment.

Parameter	Road (k=1)	Rail (k=2)
Speed (km/h)	70	100
Unit cost (CNY/t·km)	0.8	0.35
Ambient temperature (°C)	5	20
Transfer cost (CNY/t·transfer)	8.0	8.0
Transfer time (h/transfer)	2.0	2.0
Demand (t): D1 / D2	20 / 15	20 / 15
Time window (h): D1 / D2	[24,36] / [30,48]	[24,36] / [30,48]
Unit value W (CNY/t)	3,000	3,000
Refrigeration c_h (CNY/t·h)	0.5	0.5
$\theta 0$ (h^{-1}), T0 (°C), Q10	0.002, 10, 2.0	0.002, 10, 2.0
Satisfaction thresholds ($\delta 1$, $\delta 2$)	(0.02, 0.15)	(0.02, 0.15)
Satisfaction function constants (a, b)	1.0	1.0
Max transfers per route N_tr	2	2
Shelf life S_d (h): D1 / D2	60 / 60	60 / 60

4.2. Pareto Solutions and Algorithm Comparison

The first stage generates 96 and 63 feasible schemes for D1 and D2. NSGA-II obtains 100 non-dominated solutions in 0.81 s. The minimum-cost solution is 21,103.56 CNY with satisfaction 0.8274 and is rail-dominated; the highest-satisfaction solution reaches 0.9652 at 37,965 CNY and uses more refrigerated road segments. Figure 3 displays the trade-off front, and Table 4 lists representative route-mode schemes.

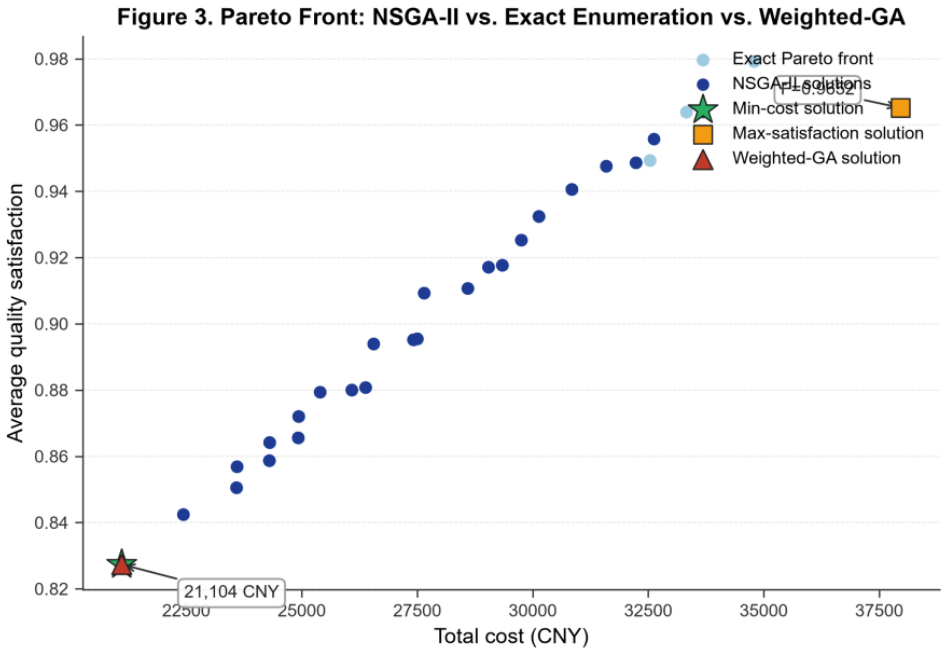


Figure 3. Pareto front from NSGA-II, exact enumeration, and weighted-GA.

Table 4. Representative Pareto-optimal schemes, with 1 = road and 2 = rail.

Scheme	Cost (CNY)	Satisfaction	Loss rate	D1 route (modes)	D2 route (modes)
1	21,103.56	0.8274	0.0849	0→2→4→5→8 (2212)	0→2→6→9 (222)
2	22,439.08	0.8424	0.0810	0→2→4→5→8 (2212)	0→2→6→9 (122)
3	22,883.74	0.8424	0.0810	0→2→4→5→8 (1212)	0→2→6→9 (222)
4	23,588.41	0.8505	0.0789	0→2→4→5→8 (2112)	0→2→6→9 (222)
5	23,599.70	0.8568	0.0772	0→2→4→5→8 (2212)	0→2→6→9 (221)
6	24,219.26	0.8575	0.0771	0→2→4→5→8 (1212)	0→2→6→9 (122)
7	24,299.87	0.8587	0.0767	0→2→4→5→8 (2211)	0→2→6→9 (222)
8	24,305.08	0.8641	0.0753	0→2→4→5→8 (2212)	0→2→6→9 (212)
9	24,923.93	0.8656	0.0750	0→2→4→5→8 (2112)	0→2→6→9 (122)
10	24,933.81	0.8720	0.0733	0→2→4→5→8 (2212)	0→2→6→9 (121)

Against exhaustive enumeration and a weighted-sum genetic algorithm, NSGA-II covers 98.0% of the exact front, matches the minimum-cost endpoint, reaches 96.8% of the exact hypervolume (0.590 versus 0.609), and gives IGD 0.0066 versus 0.696 for the single weighted-GA point. Its runtime is 0.81 s compared with 8.39 s for enumeration. The convergence of front size and average satisfaction stabilizes after about 40 generations. Figure 4 shows the convergence behavior of NSGA-II, while Table 5 summarizes the quantitative comparison among the three solution methods.

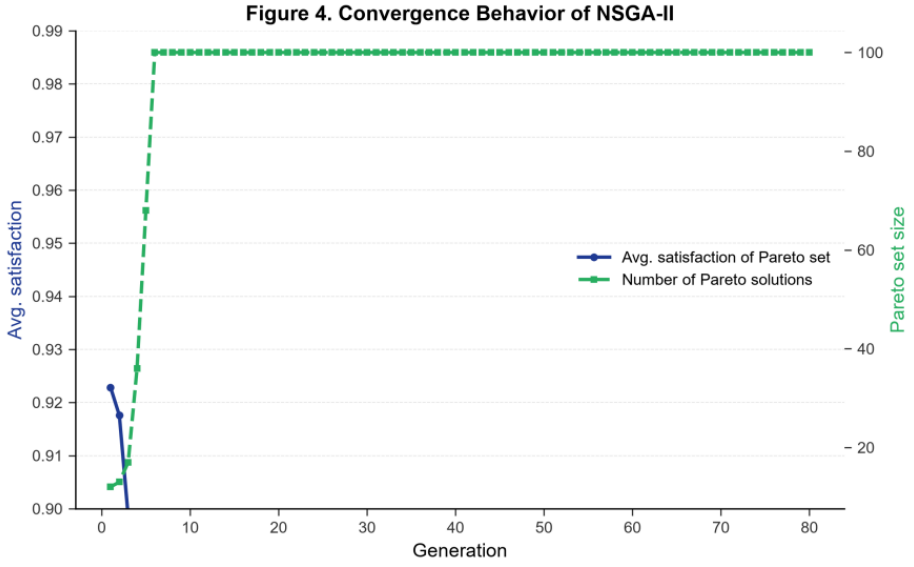


Figure 4. Convergence behavior of NSGA-II.

Table 5. Comparison of exact enumeration, NSGA-II, and weighted-GA.

Algorithm	Min cost (CNY)	Max satisfaction	Runtime (s)	Pareto size
Exact enumeration	21,103.56	0.9792	8.39	27
NSGA-II (proposed)	21,103.56	0.9652	0.81	100
Weighted-GA	21,103.56	0.8274	0.01	1 (single point)
Hypervolume (normalized)	0.609	0.590	—	—
IGD	—	0.0066	0.696	—
NSGA-II solutions matching exact front (%)	98.0			

4.3. Sensitivity To Temperature-Dependent Deterioration

The reference deterioration rate θ0 and temperature coefficient Q10 are perturbed by -20%, -10%, 0, +10%, and +20%, and NSGA-II is rerun. Increasing θ0 shifts the Pareto front toward higher cost and raises the minimum-cost loss rate from 0.0682 to 0.1014. The corresponding minimum cost ranges from 20,231 to 21,969 CNY. Changing Q10 produces a minimum-cost range of 20,310-21,899 CNY. The high-satisfaction endpoint is not monotone in Q10 because a larger temperature penalty can switch the preferred solution toward better-controlled road segments. Recent cold-chain studies likewise show that temperature-dependent quality, customer satisfaction, and exact routing constraints can change route selection [8-10]. Figures 5 and 6 illustrate the shifts of the Pareto front under changes in θ0 and Q10, respectively. Figure 7 compares the total spoilage loss of the minimum-cost solution under these parameter changes, and Table 6 summarizes the corresponding sensitivity results.

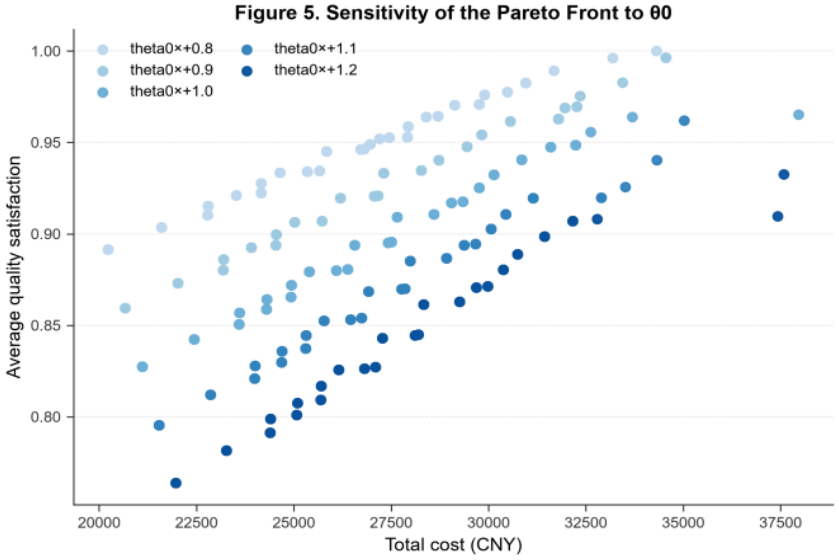


Figure 5. Sensitivity of the Pareto front to the reference deterioration rate θ0.

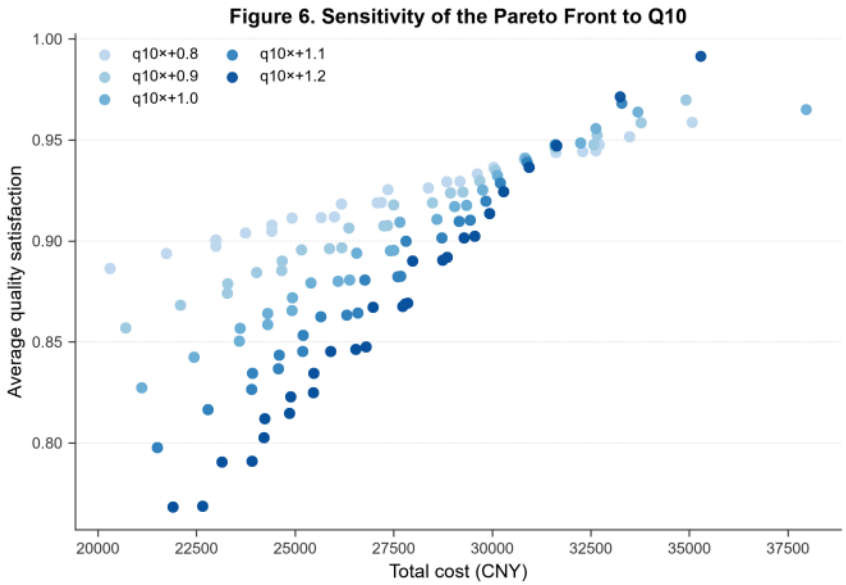


Figure 6. Sensitivity of the Pareto front to the temperature coefficient Q10.

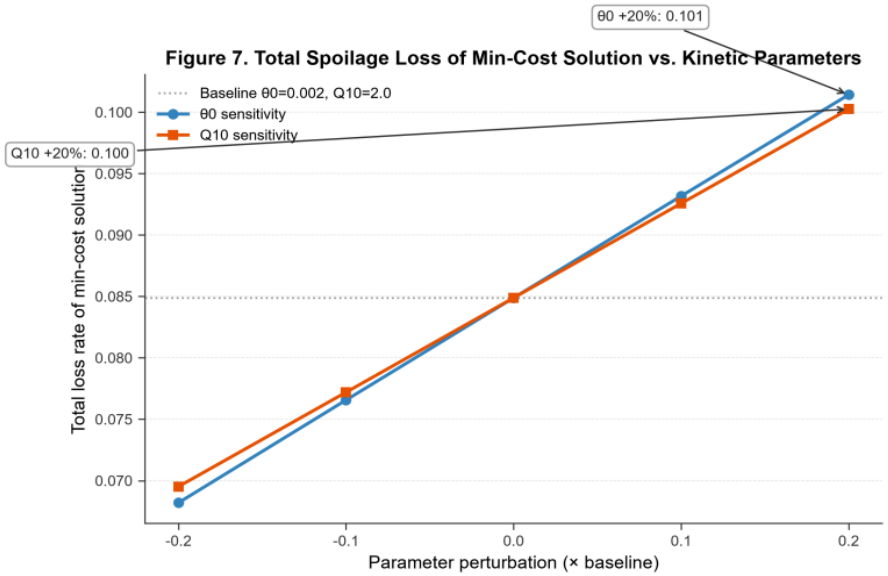


Figure 7. Total spoilage loss of the minimum-cost solution under kinetic-parameter changes.

Table 6. Sensitivity analysis of θ0 and Q10.

Scenario	Min cost (CNY)	Max satisfaction	Rail share (%)	Total loss rate
θ0 × 0.8	20,231	1.0000	90.7	0.0682
θ0 × 0.9	20,668	0.9965	90.7	0.0766
θ0 × 1.0	21,104	0.9652	90.7	0.0849
θ0 × 1.1	21,537	0.9620	90.7	0.0932
θ0 × 1.2	21,969	0.9327	90.7	0.1014
Q10 × 0.8	20,310	0.9589	90.7	0.0695
Q10 × 0.9	20,706	0.9699	90.7	0.0772
Q10 × 1.0	21,104	0.9652	90.7	0.0849
Q10 × 1.1	21,501	0.9681	90.7	0.0926
Q10 × 1.2	21,899	0.9914	90.7	0.1003

5. Conclusion

This study demonstrates the feasibility of a bi-objective multimodal routing framework that explicitly links temperature-time spoilage with transport cost and quality satisfaction. On the ten-node test network, the two-stage candidate-generation/NSGA-II method produced 100 non-dominated solutions in 0.81 s, covered 98.0% of the exact Pareto front, and reproduced the minimum-cost endpoint. The results further confirm a clear operational trade-off: rail-dominated schemes reduce monetary cost, whereas greater use of refrigerated road segments improves delivered quality. Sensitivity analysis also shows that the preferred route-mode mix responds consistently to changes in the deterioration parameters, supporting the model's use as a transparent decision aid for cold-chain planning.

The present analysis is limited by a deterministic single-supply-point network, constant mode temperatures, fixed demand and transport parameters, and validation on a relatively small synthetic network. Future research should therefore extend the framework to multiple supply points and larger real-world networks, introduce time-varying temperatures and stochastic demand or travel times, and incorporate data-driven parameter updating from actual cold-chain monitoring records. Further work can also develop adaptive or robust multi-objective algorithms to improve solution stability and computational efficiency under dynamic operating conditions.

Acknowledgement and Funding

The authors receive no financial support for the research, authorship, and publication of this article.

Declaration of Conflicting Interests

The authors declare no potential conflicts of interest with respect to the research, authorship, and/or publication of this article.

References

[1] Kim, A. N., Kim, O. W., & Kim, H. (2022). Degradation kinetics of physicochemical and sensory properties of rice during storage at different temperatures. *LWT*, 164, 113688.

[2] Liu, S. (2023). Multimodal transportation route optimization of cold chain container in time-varying network considering carbon emissions. *Sustainability*, 15, 4435.

[3] Zheng, C., Sun, K., Gu, Y., et al. (2022). Multimodal transport path selection of cold chain logistics based on improved particle swarm optimization algorithm. *Journal of Advanced Transportation*, 2022, 5458760.

[4] Li, L., Zhang, Q., Zhang, T., et al. (2023). Optimum route and transport mode selection of multimodal transport with time window under uncertain conditions. *Mathematics*, 11, 3244.

[5] Gao, L. (2025). Route optimization of multimodal transport considering regional differences under carbon tax policy. *Sustainability*, 17, 5743.

[6] Peng, Y., Zhang, Y., Yu, D. Z., et al. (2024). Multiobjective route optimization for multimodal cold chain networks considering carbon emissions and food waste. *Mathematics*, 12, 3559.

[7] Wu, D., Li, J., Cui, J., et al. (2023). Research on the time-dependent vehicle routing problem for fresh agricultural products based on customer value. *Agriculture*, 13, 681.

[8] Bei, H., Yu, M., Yang, T., & Murcio, R. (2025). Optimization of intermodal transportation routes for perishable goods considering customer satisfaction. *Research in Transportation Business and Management*, 59, 101261.

[9] Lin, N., Kanellopoulos, A., Akkerman, R., et al. (2025). Vehicle routing in precooling logistics with dynamic temperature-dependent product quality decay. *European Journal of Operational Research*, 321(2), 407–427.

[10] Hülagü, S., Ciancio, C., Dabia, S., et al. (2026). An exact algorithm for the vehicle routing problem with time windows and perishable products. *Transportation Science*.